DOI: 10.1002/ejic.201100700

Heterometallic Oximato-Bridged Linear Trinuclear $Ni^{II}-M^{III}-Ni^{II}$ (M^{III} = Mn, Fe, Tb) Complexes Constructed with the *fac*-O_3 $[Ni(HL)_3]^-$ Metalloligand (H_2L = pyrimidine-2-carboxamide oxime): A Theoretical and Experimental Magneto-Structural Study

Cerise Kalogridis,[a] María A. Palacios,[a] Antonio Rodríguez-Diéguez,[a] Antonio J. Mota,[a] Duane Choquesillo-Lazarte,[b] Euan K. Brechin,[c] and Enrique Colacio*[a]

Keywords: Magnetic properties / Heterometallic complexes / Manganese / Iron / Lanthanides / Oximate / Density functional calculations

Three oximato-bridged linear trinuclear heterobimetallic complexes of formula $[\{Ni(HL)_3\}_2M]X{\cdot}nS$ [M = Mn^{3+}, X = ClO_4^-, *n* = 9, S = H_2O (**1**); M = Fe^{3+}, X = ClO_4^-, *n* = 9, S = H_2O (**2**); M = Tb^{3+}, X = NO_3^-, *n* = 11, S = CH_3OH (**3**); H_2L = pyrimidine-2-carboxamide oxime] were prepared from the reaction of the in situ generated $[Ni(HL)_3]^-$ complex with the corresponding M^{2+} salts for **1** and **2** (which are oxidized to M^{3+} during the course of the reaction) and the Tb^{3+} salt for **3**. The heterometallic trinuclear $[NiMNi]^+$ cationic entities are formed by the coordination of two $[Ni(HL)_3]^-$ metalloligands to the central M^{3+} metal ion through three facially arranged oxime oxygen atoms belonging to the H_2L ligands. Therefore the HL^- ligand acts in a κ^2-N_1,N_8:κ-O_9 bidentate bridging mode. Compounds **1** and **2** exhibit antiferromagnetic interactions, whereas for **3** the spin-orbit coupling and the effects of the crystal-field on the $^{2S+1}L_J$ states of the Tb^{3+} ion encumbers the determination of the nature of the magnetic exchange interaction between the Ni^{2+} and Tb^{3+} ions through the oximato bridging group. DFT calculations carried out on the solid-state structures predict *J* values that match well with the experimental ones. The experimental *J* values were compared with those observed for analogous NiMNi complexes and their differences justified on the basis of structural parameters such as the Ni–N–O–M torsional angle and the distortion from the OC-6 octahedral to the TPR-6 trigonal prismatic geometry.

Introduction

Oxime ligands have been extensively investigated not only due to their great ability to form homo- and heterometallic 3D polynuclear complexes but also due to the interesting magnetic properties they can transmit.[1] Among them, R-substituted 2-pyridyloximes, (py)C(R)NOH, and salicylaldoximes, R-saoH_2, play an outstanding role since they are able to generate a great variety of polynuclear complexes with aesthetically pleasing structures and interesting magnetic properties, including Single Molecule Magnet (SMM)[1c,2] and Single Chain Magnet (SCM) behaviour.[3] It should be noted that the coordination chemistry of (py)C(R)NOH ligands, in which the R group is replaced by an amino donor group remains largely unexplored. Except for a dodecanuclear Ni_{12} cluster,[4] where the (py)C(NH_2)NOH ligand adopts four different anionic chelating/bridging coordination modes, and some Ni_4, Ni_8 and Ni_{12} multi-decker complexes based on $[Ni_4]^{2+}$ units bearing two chelating/bridging tridentate [μ-(py)C(NH_2)NO]$^-$ ligands and two bis(chelating)/bridging pentadentate [μ_3-(py)C(NH)NO]$^{2-}$ ligands,[4a,4b] all the reported complexes are mononuclear with the ligand coordinating in a chelating neutral form through both the heterocyclic and oxime nitrogen atoms.[1b] Single-decker as well as a 2D complexes based on the $[Ni_4]^{2+}$ unit have also been obtained with the pyrazine-2-carboxamido oxime ligand.[4d] Recently we,[5] and others,[6] have begun to use the analogous ligand pyrimidine-2-carboxamide oxime (H_2L) for the synthesis of polynuclear complexes. It is expected that the difference in electronic properties and capability of establishing hydrogen bonds promoted by the presence of an extra endocyclic nitrogen in the sixth position of the pyrimidine ring in H_2L may modify its coordination properties with respect to those of the pyridine analogue and, as a consequence, eventually afford polynuclear complexes with either different structures and/or magnetic properties. The first results along this line show that homo- and heterometallic tetranuclear Ni_4,[5] Ni_2Cu_2[6] and Cu_4[6] complexes can be obtained, where HL^- and L^{2-} adopt the coordination modes given in Scheme 1.

[a] Departamento de Química Inorgánica, Universidad de Granada,
Av. Fuentenueva s/n, 18071 Granada, Spain
[b] Laboratorio de Estudios Cristalográficos, IACT-CSIC, 18100, Granada, Spain
[c] School of Chemistry, The University of Edinburgh, West Mains Road, Edinburgh, EH9 3JJ, United Kingdom
Supporting information for this article is available on the WWW under http://dx.doi.org/10.1002/ejic.201100700.

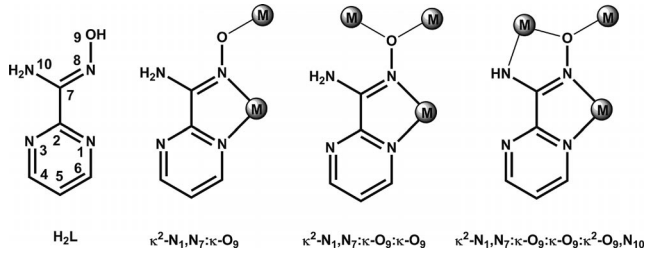

Scheme 1. Coordination modes of the H_2L ligand in polynuclear complexes.

It has been shown that the pyridine-2-aldoxime ligand is able to form the tris(pyridine-2-aldoximato)nickel(II) mononuclear anionic complex, which can be used itself as a "complex ligand" to generate homo- and heteronuclear complexes.[7] In light of this, we decided to use the in situ generated $[Ni(HL)_3]^-$ complex which should exhibit three free donor oxime oxygen atoms in a *fac* disposition, as a metalloligand for the preparation of heteronuclear oximate-bridged complexes. In this paper we report on the synthesis, structure, magnetic properties and DFT calculations of the oximato-bridged trinuclear complexes of general formula $[\{Ni(HL)_3\}_2M]X{\cdot}nS$ [M = Mn^{3+}, X = ClO_4^-, *n* = 9, S = H_2O (**1**); M = Fe^{3+}, X = ClO_4^-, *n* = 9, S = H_2O (**2**); M = Tb^{3+}, X = NO_3^-, *n* = 11, S = CH_3OH (**3**)].

Results and Discussion

The use of "metal complexes as ligands" has been shown to be a good strategy for the preparation of triply oximato-bridged polynuclear complexes. Thus, neutral *fac* or *mer* $[Co^{III}\{(py)C(R)NOH\}_3]$ complexes[8] (R = H, Me or Ph) as well as the neutral *fac* $[Ni^{II}\{(py)C(Me)NO\}_2\{(py)C(Me)NOH\}]$ complex[9] have been successfully used as metalloligands for the formation of $Co^{III}-Co^{II}-Co^{III}$ and $Ni^{II}-Tb^{III}-Ni^{II}$ linear trinuclear complexes, respectively. For the preparation of the analogous $Ni^{II}-M^{III}-Ni^{II}$ complexes (M^{III} = Mn, Cr, Fe), however, the in situ generated $[Ni\{(py)C(H)NO\}_3]^-$ anion was used.[7] Following this latter strategy, we have carried out the reaction of a solution of the corresponding Ni^{2+} salt, H_2L and triethylamine in 1:3:3 molar ratio mixture (metalloligand solution) with $M(ClO_4)_2{\cdot}6H_2O$ (M = Mn^{2+} and Fe^{2+}) in the cases of **1** and **2**, respectively, and $Tb(CF_3SO_3)_3$ in the case of **3**, using a 1:1 metalloligand/M^{2+} molar ratio. It should be noted that the TOF MS ESI^+ spectrum of the metalloligand solution actually shows that the most abundant species in solution is $[Ni(HL)(H_2L)]^+$ (*m*/*z* = 333). The 1:1 molar ratio was used instead of a 2:1 ratio in an attempt to cover a wider range of potential oximato-bridged polynuclear species. However, the reaction with a second metal ion (M or Tb) always evolves towards the heterobimetallic *fac*-O_3 oximato-bridged trinuclear complexes. Note that the Mn^{2+} and Fe^{2+} ions are oxidised to Mn^{3+} and Fe^{3+} in the course of the formation of compounds **1** and **2**, respectively. The same oxidation processes were observed in the formation of the analogous complexes containing the pyridine-2-aldoximato ligands.[7] It should be noted at this point that compounds **1**–**3** can be alternatively obtained as crystals by using a 2:1 metalloligand/M molar ratio but the yield based on Ni^{II} does not improve with respect to that obtained when a 1:1 metalloligand/M molar ratio was used. Although all attempts to grow crystals of salts containing the $[Ni(HL)_3]^-$ metalloligand failed, however, we succeeded in obtaining the *fac* mononuclear complex $[Ni(H_2L)_3]^{2+}$ (see Supporting Information). The reaction of this metalloligand with either M^{II} (M = Mn, Fe) or Tb^{III} in methanol and using triethylamine as a base led to the precipitation of compounds, the elemental analyses and IR spectra of which match with those expected for $[\{Ni(HL)_3\}_2M^{III}]X$ species analogous to **1**–**3**. Despite our great efforts we could not grow crystal of these compounds suitable for X-ray crystallography.

Crystal Structures

Compounds **1** and **2** are isomorphous and their structures consist of linear $[NiMNi]^+$ cationic entities, one perchlorato anion and nine crystallisation water molecules. The structure of **3** is similar to that of **1** and **2** but it consists of centrosymmetric linear $[NiTbNi]^+$ cationic units, one nitrato anion and eleven crystallisation methanol molecules. Within the cationic heterometallic trinuclear entities two $[Ni(HL)_3]^-$ metalloligands, acting as tridentate ligands, are connected to the central M^{3+} metal ion through three facially arranged oxime oxygen atoms belonging to the H_2L ligands. A view of the $[NiMNi]^+$ cation present in complexes **1** and **2** is shown in Figure 1 and the structure of **3** is given in Figure 2.

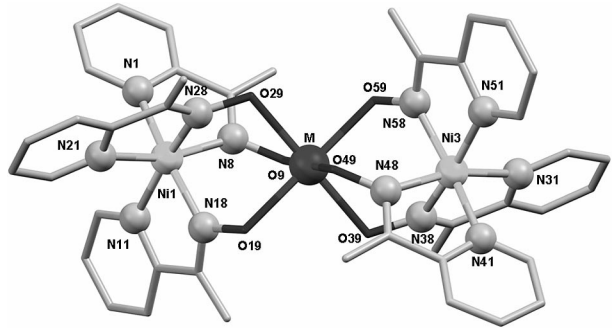

Figure 1. Perspective view of the structure common to complexes **1** and **2** and atom numbering scheme. The perchlorato counteranion and hydrogen atoms are omitted for the sake of clarity.

The Ni^{2+} ions exhibit distorted octahedral NiN_6 coordination environments, the distortion being mainly due to the small bite of the HL^- ligand (approximately 77°). The calculation of the degree of distortion of the Ni coordination polyhedron with respect to ideal six-vertex polyhedra, by using the continuous shape measure theory and SHAPE software,[10] led to shape measures relative to the octahedron (OC-6) and trigonal prism (TPR-6) with values of 2.358 and 8.775 for **1**, 2.317 and 8.909 for **2**, and 1.639 and 10.90 for **3**, respectively. Therefore, the NiN_6 coordination

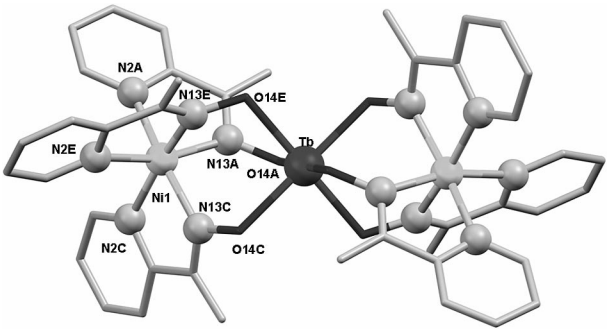

Figure 2. Perspective view of the structure of **3** and atom numbering scheme. The nitrato anion and hydrogen atoms have been omitted for the sake of clarity.

spheres can be considered as octahedral but somewhat distorted towards trigonal prismatic. The shape measures relative to other reference polyhedra are significantly larger. Tris(bidentate) NiN_6 units, which display opposite propeller-like chirality (Δ and Λ), are formed by the coordination of three pyridine nitrogen atoms (N_{py}) and three oxime nitrogen atoms (N_{ox}) belonging to the three HL^- ligands. Therefore, the HL^- ligands exhibit a κ^2-N_1,N_8:κ-O_9 bidentate bridging mode. The Ni–Npy bond lengths are about 0.1 Å longer than the Ni−N_{ox} ones, which are close to 2 Å. In general, these Ni–N bond lengths are similar to those observed for analogous complexes with the pyridine-2-aldoximato ligand.[7] As expected for this type of oximato-bridged complex, the chelate rings are planar whereas the M–O–N–Ni bridging fragments are not, with M–O–N–Ni torsional angles in the ranges 39.19–49.43°, 38.34–47.24° and 41.96–46.45° for **1**, **2** and **3**, respectively.

The M^{3+} central ions exhibit MO_6 coordination spheres with almost perfect octahedral geometry with respect to the bond angles since the shape measures relative to the octahedron (OC-6) are 0.494 for **1**, 0.207 for **2** and 0.071 for **3**, whereas the next values, that correspond to the trigonal prismatic polyhedron (TPR-6), are larger than 15. As expected for a high spin d^4 ion, the MnO_6 coordination sphere exhibits Jahn–Teller tetragonally elongated distortion along the O_{49}–Mn–O_9 axis with Mn–O_{49} and Mn–O_9 bond lengths of 2.139 Å and 2.167 Å. The bond lengths in the equatorial plane are in the range of 1.952–1.973 Å. In contrast to **1**, the analogous complex containing the pyridine-2-aldoximato ligand[7] exhibits perfect octahedral geometry which has been justified by the possible existence of a dynamic Jahn–Teller effect.[11] In the case of **2**, all the Fe–O bond lengths in the FeO_6 coordination sphere are found in a short range (2.009–2.060 Å) as expected for a high spin d^5 ion that is not subjected to Jahn–Teller distortion. It should be noted that the TbO_6 coordination sphere observed in **3** is infrequently found in Tb^{3+} complexes[9,12] because higher coordination numbers are usually preferred. The adoption of the octahedral TbO_6 coordination sphere may be due, among other reasons, to the larger lattice energies for this highly symmetric geometry in comparison with some of the seven, eight or nine vertex polyhedra.[12] The Tb–O distances in the centrosymmetric TbO_6 coordination polyhedron are found in the range 2.276–2.295 Å and are similar to that observed in the analogous complex with the pyridine-2-aldoximato bridging ligand. The average Mn–Ni and Fe–Ni bond lengths for **1** and **2** and the Tb–Ni distance for **3** are 3.605, 3.608 and 3.689 Å, respectively.

The trinuclear molecules are involved in extended hydrogen-bonding networks, in which the amino group, the uncoordinated pyrimidine nitrogen atom, the solvent molecules and the counteranions all participate.

Magnetic Properties

The temperature dependencies of χ_M and $\chi_M T$ for complex **1** (χ_M is the molar magnetic susceptibility per Ni^{II}-$Mn^{III}Ni^{II}$ unit) in an applied magnetic field of 0.5 T are displayed in Figure 3.

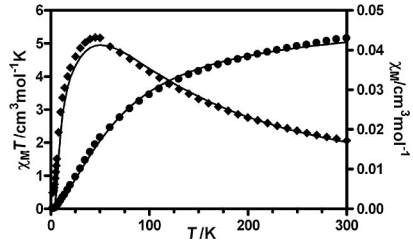

Figure 3. Temperature dependencies of $\chi_M T$ and χ_M for **1**.

The value of $\chi_M T$ at room temperature (5.16 $cm^3 K mol^{-1}$) matches well with that expected for two uncoupled Ni^{2+} ions (g = 2, S = 1) and one uncoupled Mn^{3+} ion (g = 2, S = 2) of 5 $cm^3 K mol^{-1}$. The $\chi_M T$ product shows a continuous decrease with decreasing temperature to reach a value of 0.008 $cm^3 K mol^{-1}$ at 2 K which points out the presence of antiferromagnetic interactions between the central Mn^{3+} ion and the external Ni^{2+} ions. In keeping with this, the thermal variation of χ_M shows a broad maximum near 40 K. Simulation of the magnetic susceptibility data with the Hamiltonian $H = -J(S_{Mn}S_{Ni1} + S_{Mn}S_{Ni2})$ and using the MAGMUM[13] program yielded an average g = 2.17(6) and a J = –19.3(3) cm^{-1} (the interaction between the external Ni^{2+} ions was considered to be negligible). The interaction mainly takes place through the σ pathway involving the sp^2 orbitals of the oximato N and O atoms and the e_g type orbitals on the Mn^{3+} and Ni^{2+} ions. The antiferromagnetic interaction found for $Ni^{II}Mn^{III}Ni^{II}$ (**1**) agrees well with that observed for a $Mn^{III}Ni^{II}$ complex in which the metal ions are bridged by three pyridine-2-aldoximato ligands using the same coordination mode as in complex **1**.[14] However, it is rather stronger than that observed for the analogous $Ni^{II}Mn^{III}Ni^{II}$ complex bearing pyridine-2-aldoximato ligands.[7a]

The stronger AF interaction observed for **1** with respect to the corresponding HL_1-based complex may be attributed to: (i) the presence of the extra amino group in the oximato ligand of complex **1** that delocalises its electronic density toward the oximato bridging group and (ii) the distortion from OC-6 to TPR-6 of the NiN_6 coordination environment of **1** (see Table 1) is smaller than that observed in the

Table 1. Structural and magnetic data for NiMNi tris(oximato)-bridged linear complexes.

	Reference	$J_{exp.}$ /cm^{-1}	$J_{calcd.}$ /cm^{-1}	M–O–N–Ni /°	% OC-6 Ni	M
1	this work	–19.3 (3)	–20.4	43.88	71.9 (8.2)[a]	94.9 (11.6)[a]
2	this work	–30.1(5)	–34.0	42.84	71.4 (5.7)[a]	94.9 (7.9)[a]
{[Ni(L$_1$)$_3$]$_2$Mn}(ClO$_4$)	[7a]	–6.3	+12.2	36.54	67.2 (5.1)[a]	99.1 (10.4)[a]
{[Ni(L$_1$)$_3$]$_2$Fe}(ClO$_4$)	[7b]	–57.0	–58.6	38.37	70.8 (5.1)[a]	99.2 (10.4)[a]

[a] Deviation from the OC-6↔TPR-6 deformation pathway. HL_1 = pyridine-2-aldoxime.

analogous complex containing pyridine-2-aldoximato ligands (28.1% compared with 32.8%). It has been pointed out that AF interactions increase as the distortion decreases.[7] The Ni–N–O–Mn torsional angle (α) should also play an important role in determining the magnitude of the magnetic exchange interaction between the metal magnetic orbitals through the NO bond. In principle, for Ni–N–O–M pathways involving the same type of magnetic orbital on each metal ion (for instance $d_{x^2-y^2}$) the following magneto-structural correlation would be expected: the larger the Ni–N–O–M angle, the lower the antiferromagnetic interaction. In accordance with this correlation, experimental and theoretical studies on oximato-bridged dinuclear Ni^{II} systems have clearly shown that the magnetic exchange interaction decreases with the increase of the α angle as the overlap between the sp^2 orbitals of the oxime N and O atoms on either side of the bridging oximato group becomes smaller.[5] However, compound **1** and the analogous complex containing pyridine-2-aldoximato ligands do not follow this correlation. The smaller average Mn–O–N–Ni torsion angle for the latter compound (36.54°) compared to **1** (43.88°) should favour a stronger magnetic exchange interaction in the former which is in clear contrast with the experimental observation. The different mutual orientation of the Ni^{2+} and Mn^{3+} magnetic orbitals for **1** and the analogous complex containing pyridine-2-aldoximato ligands might be the reason why the magnetic exchange interaction is stronger for **1** in spite of having a higher torsional angle. Because the mutual orientation of the Ni^{2+} and Mn^{3+} magnetic orbitals is directly related to the distortion of their respective coordination spheres, it seems that in this case the effect of points (i) and (ii) on the magnetic exchange interaction would be more important than the effect promoted by the Mn–O–N–Ni torsional angle. Nevertheless, more examples of oximato-bridged Ni–Mn complexes are needed to evaluate the relative effect of the α angle and the orientation of the magnetic orbitals on the magnetic exchange interaction.

The magnetic properties of compound **2** in the form of the temperature dependencies of χ_M and $\chi_M T$ (χ_M is the molar magnetic susceptibility per Ni^{II}Fe^{III}Ni^{II} unit) in an applied magnetic field of 0.5 T are shown in Figure 4. The $\chi_M T$ product at room temperature (5.33 cm^3 K mol^{-1}) is smaller than that expected for two uncoupled Ni^{2+} ions (g = 2, S = 1) and one uncoupled Fe^{3+} (g = 2, S = $^5/_2$) of 6.375 cm^3 K mol^{-1} which is probably due to the existence of moderate to strong antiferromagnetic exchange interaction between Ni^{2+} and Fe^{3+} metal ions mediated by the oximato bridges. The $\chi_M T$ product shows a continuous decrease with decreasing temperature reaching a plateau at about 10 K with a value of 0.41 cm^3 K mol^{-1}. This behaviour thus supports the presence of antiferromagnetic interactions between the metal ions leading to an S_T = ½ doublet ground state. In keeping with this, the thermal variation of χ_M shows a broad maximum near 60 K and, below this temperature, χ_M decreases to reach a minimum at 25 K and then increases to a value of 0.20 cm^3 K mol^{-1} at 2 K. The increase at low temperature corresponds to the Curie law for an S = ½ paramagnetic system.

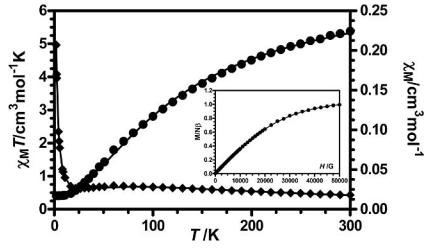

Figure 4. Temperature dependencies of $\chi_M T$ and χ_M for **2**. Inset: M vs. T plot.

The field dependence of the magnetisation at 2 K is given in the inset of Figure 4. The value of the magnetisation at the maximum applied field of 5 T is 0.99 Nβ and this matches well with the expected value for S = ½ thus supporting the nature of the ground state. The magnetisation data fit well to the Brillouin function with g = 2.1 and S = ½.

The experimental susceptibility data were simulated with the above indicated Hamiltonian and the following parameters: g = 2.11(2) and J = –30.1(5) cm^{-1}. The magnetic exchange coupling in **2** is smaller than that reported for the analogous trinuclear Ni^{II}Fe^{III}Ni^{II} complex containing pyridine-2-aldoximato ligands[7b] of –57 cm^{-1} (see Table 1). Since the distortion of the NiN$_6$ chromophore from OC-6 to TPR-6 for both compounds is very similar (28.6% for **2** and 29.2% for its analogue), the difference in the magnitudes of their respective magnetic exchange couplings may be mainly attributed to the fact that the average Fe–O–N–Ni torsional angle for **2** of 42.48° is bigger than that of 38.37° observed for the analogous complex containing pyridine-2-aldoximato ligands.

In order to support the experimental values of J for compounds **1** and **2**, DFT calculations were carried out on their X-ray structures as found in the solid state. Likewise, the J values for the analogous complexes bearing the pyridine-2-

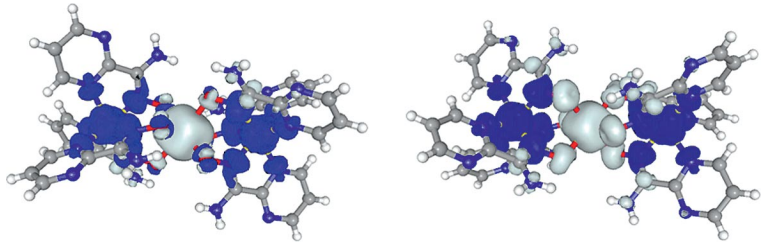

Figure 5. Calculated spin density distribution for the broken-symmetry singlet state of **1** (left) and doublet state **2** (right). Positive and negative values are represented as grey and black surfaces, respectively. The isodensity surfaces represented correspond to cut-off values of 0.0020 e Bohr^{-3}.

aldoxime ligand were also calculated. The calculations predict J values for **1** and **2** that match well with that obtained from the experimental susceptibility data (see Table 1). The calculated magnetic exchange interactions between the external Ni^{2+} ions (J') are negligible, which justifies the assumption of a $J' = 0$ value for experimental susceptibility data fitting. It should be noted that there is a large difference between the experimental and calculated J values for $\{[Ni(L_1)_3]_2Mn\}(ClO_4)$.[7a] We have not yet found a reasonable explanation for such a difference between both values.

The calculated spin density for the ground BS (broken symmetry) singlet and doublet states for **1** and **2**, respectively, are given in Table 2 (the spin density distributions for these complexes are shown in Figure 5) and offer information on the electronic structure and the mechanism of the magnetic exchange interaction.

Table 2. Spin densities for complexes **1** and **2**.

Atoms/spin densities	Complex **1**	Complex **2**
Ni	–1.6163	–1.6153
Mn[a], Fe	+3.8898	+4.1701
Ni	–1.6124	–1.6132
O[b]	O_{eq} –0.0320/O_{ax} +0.0013[c]	+0.0852
N_{oxim}[b]	N_{eq} –0.0822/N_{ax} –0.1094[c]	–0.1089
N_{pyrim}[b]	N_{eq} –0.0399/N_{ax} –0.0368[c]	–0.0357

[a] Mn for complex **1** and Fe for complex **2**. [b] Mean values. [c] There are equatorial and axial positions because of the Jahn–Teller effect operating on the Mn^{III} complex.

As expected, the spin density distributions show the predominance of the delocalisation mechanism through a σ type exchange pathway involving the e_g magnetic orbitals of the Ni^{2+} ions and the sp^2-hybrid orbitals of the oxygen and nitrogen oxime atoms.

The shapes of the spin density for Mn^{3+} and Fe^{3+} ions are cubic and quasi spherical as expected for sets of four and five d orbitals, respectively, with one unpaired electron on each. The spin densities are somewhat flattened in the directions of the metal-ligand bonds. This loss of sphericity at the Mn^{3+} and Fe^{3+} ions is the result of the smaller spin density at the e_g orbitals than at the t_{2g} orbitals which is a consequence of the significant spin density delocalisation for the σ type e_g orbitals to the donor atoms of the ligand. The spin density delocalised on the oxygen atoms of the bridging region, in absolute value, is significantly smaller than those on the oxime nitrogen atoms (N_{ox}). In any case, the spin density is mainly found at the metal, as expected if they are the magnetic centres. The relatively small spin density delocalised on the oxime bridging oxygen atoms reflects the moderate antiferromagnetic interaction observed for these compounds. It should be noted that the spin density delocalised on the oxime oxygen atoms in **2** is higher than in **1** which is in agreement with the fact that compound **2** exhibits a stronger AF coupling.

The temperature dependence of the $\chi_M T$ product for **3** at 0.1 T is given in Figure 6. The room temperature $\chi_M T$ value of 11.74 cm^3 K mol^{-1} is slightly low but still in relatively good agreement with the expected value (13.8 cm^3 K mol^{-1}) for two Ni^{II} ($S = 1$, $C = 1$ cm^3 K mol^{-1}) and one Tb^{3+} metal ion ($S = 3$, $L = 3$, $^7F_6$, $g = {}^3/_2$, $C = 11.815$ cm^3 K mol^{-1}) in the free-ion approximation.[15] The $\chi_M T$ product decreases continuously on lowering the temperature, first slowly to 100 K and further sharply to reach a value of 5.41 cm^3 K mol^{-1} at 5 K. Similar magnetic behaviour has been observed for the analogous complex containing the pyridine-2-aldoximato ligand.[9]

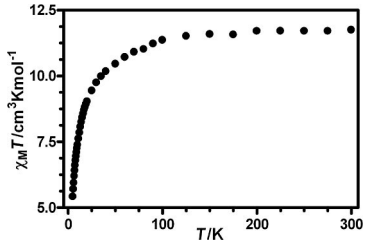

Figure 6. Temperature dependence of of $\chi_M T$ for **3**.

In Ln^{3+} complexes, the interelectronic repulsions and the spin-orbit coupling give rise to $^{2S+1}L_J$ states, which in turn are split further into Stark components by crystal-field effects of the order of 100 cm^{-1}. The number of Stark sublevels arising from the ground state depends on the crystal-field symmetry[12] (Figure 7).

At room temperature, all the ground state Stark sublevels are statistically populated and the free-ion approximation applies. However, when the temperature is lowered, the depopulation of these sublevels leads to a deviation of the $\chi_M T$ product from the Curie law.[16] Moreover, because the magnetic exchange constants are expected to be weak for 3d-4f systems,[17] the decrease of the $\chi_M T$ product in this compound is mainly due to the depopulation of the Stark sublevels and not to the magnetic exchange interactions. This behaviour encumbers the determination of the nature

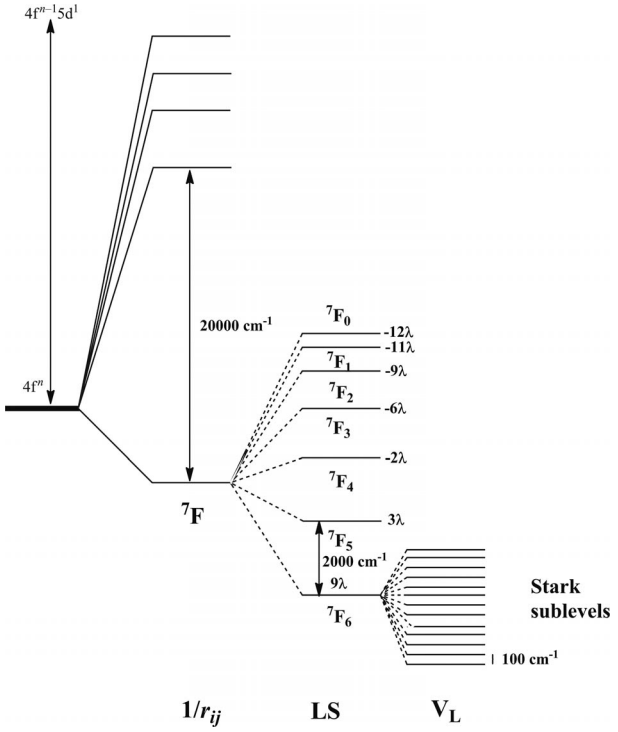

Figure 7. Splitting of the ^7F ground term of Tb^{3+} by spin-orbit and crystal-field interactions.

of the magnetic exchange interaction between Ni^{2+} and Tb^{3+} ions through the oximato bridging group. The local effects of the Tb^{3+} cation due to the depopulation of the Stark sublevels could be evaluated by comparing the magnetic properties of **3** with those of the isostructural compound Zn_2Tb. However, all attempts to obtain this compound failed. Previous investigations on isostructural $Ni^{2+}-Ln^{3+}$ complexes have shown that Gd^{III} and Tb^{III} compounds display magnetic-exchange interactions of the same nature (generally ferromagnetic).[15] In view of this, we decided to prepare the isostructural Ni_2Gd compound to indirectly obtain information about the Tb−Ni interactions. However, also in this case, all the efforts to grow crystals of the Ni_2Gd complex, either by following the same method as for compound **1**–**3** or by using a step-by-step strategy starting from the isolated $[Ni(H_2L)_3]^{2+}$ metalloligand, were unsuccessful.

Since Tb^{3+} is a highly anisotropic ion, compound **3** might be a good candidate for displaying slow relaxation of the magnetisation and single-molecule magnet (SMM) behaviour. However, the ac susceptibility in zero dc field shows a complete absence of an out-of-phase component above 1.8 K. It has been demonstrated that an axial ligand-field induces a strong Ising-type anisotropy of the Tb^{3+} ion, thus favouring SMM behaviour.[18] Therefore, the absence of SMM behaviour may be related with the high symmetry around Tb^{3+} with almost a perfect O_h geometry. As far as we know, only one example of SMM involving a LnO_6 coordination environment has been reported so far.[19] It corresponds to a Dy_5 cluster where the Dy ions exhibit a distorted octahedral geometry with C_{4v} symmetry.

It is well known that 3d-4f[20]and even 4f[19,21] complexes containing Dy^{3+} are found among the best candidates for exhibiting SMM behaviour. In view of this we decided to prepare the Ni_2Dy complex. However, in this case, our intense efforts to grow crystals suitable for X-ray crystallography also failed.

Concluding Remarks

We have successfully prepared three oximato-bridged linear trinuclear heterometallic complexes using the "complex as ligand" strategy. Thus, the reaction of the in situ generated $[Ni(HL)_3]^-$ complex ligand with the corresponding M^{2+} salt afforded the complexes $\{[Ni(HL)_3]_2M\}X$ (M = Mn^{3+}, X = ClO_4^- **1**, M = Fe^{3+}, X = ClO_4^- **2** and M = Tb^{3+}, X = NO_3^- **3**; H_2L = pyrimidine-2-carboxamide oxime). Compounds **1** and **2** exhibit antiferromagnetic interactions between the Ni^{2+} and M^{3+} ions through the oximato bridging groups and their *J* values match well with those calculated from DFT methods. Compared with the analogous complexes bearing the pyridine-2-aldoximato ligand, **1** and **2** exhibit both larger Ni–N–O–M angles and higher distortions from the octahedral to the trigonal prismatic geometry. These structural differences (which could be promoted by the different capability for establishing hydrogen bonding promoted by the presence of an amino group and an extra endocyclic nitrogen in sixth position of the pyrimidine ring in H_2L compared to the pyridine-2-aldoximato ligand), together with the different electronic properties of the ligands would justify the different antiferromagnetic coupling observed for **1** and **2** and their analogous pyridine-2-aldoximato containing complexes. For **3**, the spin-orbit coupling and the effects of the crystal-field on the $^{2S+1}L_J$ states of the Tb^{3+} ion hampers the determination of the nature of the magnetic exchange interaction between the Ni^{2+} and Tb^{3+} ions through the oximato bridging group.

Experimental Section

General: Unless stated otherwise, all reactions were conducted in oven-dried glassware in aerobic conditions, with the reagents purchased commercially and used without further purification. The ligand H_2L was prepared as described previously.[22]

$\{[Ni(HL)_3]_2Mn\}(ClO_4)\cdot 9H_2O$ (1): To a solution of H_2L (0.080 g, 0.58 mmol) in a methanol/water (1:1) mixture (30 mL) were added successively with continuous stirring triethylamine (0.1 mL, 1 mmol) and $Ni(ClO_4)_2\cdot 6H_2O$ (0.050 g, 0.14 mmol). After 15 min, a solution of $Mn(ClO_4)_2\cdot 6H_2O$ (0.053 g, 0.14 mmol) in methanol/water (1:1, 10 mL) was added to the reaction mixture. The resultant deep-brown solution kept at room temperature for a week afforded block-like black crystals suitable for X-ray diffraction. Crystals were filtered, washed with methanol and air-dried; yield 52%. $C_{30}H_{48}ClMnN_{24}Ni_2O_{19}$ (1256.67): calcd. C 28.67, H 3.85, N 26.75; found C 29.12, H 3.56, N 26.75. IR (KBr): $\tilde{\nu}$ = 3399 $\nu(NH_2)$ + ν(OH); 1638, ν(C=C); 1467, ν(CN); 1083 $\nu(ClO_4)$ cm^{-1}.

$\{[Ni(HL)_3]_2Fe\}(ClO_4)\cdot 9H_2O$ (2): This compound was prepared by using the same method as for **1** but using $Fe(ClO_4)_2\cdot H_2O$ (0.036 g, 0.14 mmol) instead of $Mn(ClO_4)_2\cdot 6H_2O$. Deep brown crystals suit-

able for X-ray diffraction were obtained; yield 43%. $C_{30}H_{48}ClFeN_{24}Ni_2O_{19}$ (1257.58): calcd. C 28.65, H 3.85, N 26.73; found C 29.09, H 3.72, N 26.73. IR (KBr): $\tilde{\nu}$ = 3447 $\nu(NH_2)$ + ν(OH); 1638, ν(C=C); 1465, ν(CN); 1086 $\nu(ClO_4)$ cm^{-1}.

{[Ni(HL)$_3$]$_2$Tb}(NO$_3$)·11CH$_3$OH (3): To a solution of H_2L (0.100 g, 0.73 mmol) in methanol (25 mL) were added successively with continuous stirring triethylamine (0.1 mL, 1 mmol) and a solution of $Ni(NO_3)_2{\cdot}6H_2O$ (0.053 g, 0.18 mmol) in methanol (5 mL). After 15 min, a solution of $Tb(CF_3SO_3)$ (0.110 g, 0.18 mmol) in methanol (5 mL) was added to the mixture and this was stirred for 30 min. The resultant orange solution kept at room temperature for a week afforded dark orange crystals suitable for X-ray diffraction. Crystals were filtered, washed with methanol and air-dried; yield 10%. $C_{41}H_{74}N_{25}Ni_2O_{20}Tb$ (1513.54): calcd. C 32.54, H 4.93, N 23.14; found C 32.14, H 5.39, N 22.73. IR (KBr): $\tilde{\nu}$ = 3415 $\nu(NH_2)$; 1637, ν(C=C); 1473, ν(CN); 1385 $\nu(NO_3^-)$ cm^{-1}.

Caution! *Although we experienced no difficulties with the compounds isolated as their perchlorato salts, the unpredictable behaviour of these salts requires extreme caution in their handling.*

Computational Details: All theoretical calculations were carried out at the DFT level of theory using the hybrid B3LYP exchange-correlation functional,[23] as implemented in the *Gaussian 03* program.[24] A quadratic convergence method was employed in the SCF process.[25] The triple ζ quality basis set proposed by Ahlrichs and coworkers was used for all atoms.[26] Calculations were performed on the complexes built from the experimental geometries. The electronic configurations used as starting points were created using *Jaguar 7.6* software.[27] The approach used to determine the exchange coupling constants for polynuclear complexes has been described in detail elsewhere.[28]

Physical Measurements: Elemental analyses were carried out at the "Centro de Instrumentación Científica" (University of Granada) on a Fisons–Carlo–Erba analyser model EA 1108. The IR spectra on powdered samples were recorded with a ThermoNicolet IR200 FTIR by using KBr pellets. Magnetisation and variable temperature (2–300 K) magnetic susceptibility measurements on polycrystalline samples were carried out with a Quantum Design SQUID MPMS XL-5 device operating at different magnetic fields. The experimental susceptibilities were corrected for the diamagnetism of the constituent atoms by using Pascal's tables.

Single-Crystal Structure Determination: Suitable crystals of **1**–**3** were mounted on glass fibres and used for data collection. Data were collected with a Bruker X8 Proteum (**1** and **2**) diffractometer at 100(2) K and 120(2) K, respectively, and with a dual source Oxford Diffraction SuperNova diffractometer (**3**) equipped with an Atlas CCD detector and an Oxford Cryosystems low temperature device operating at 100 K. Cu-K_α radiation (λ = 1.5418 Å) was used to collect data for **1** and **2** whereas Mo-K_α radiation (λ = 0.71073 Å) was used for **3**. The data of **1** and **2** were processed with APEX2[29] and corrected for absorption using SADABS.[30] Semi-empirical (multi-scan) absorption corrections were applied for **3** using *Crysalis Pro*.[31] The structures were solved by direct methods[32] and refined with full-matrix least-squares calculations on F^2.[33] The $NiTbNi^+$ cations were well resolved in the structure of **3** but the counter anions and solvent molecules were not. Instead, a new set of F^2 (*hkl*) values with the contribution from solvent molecules and nitrato anions withdrawn were obtained by the *SQUEEZE* procedure implemented in *PLATON_94*.[34] Anisotropic temperature factors were assigned to all atoms except the hydrogen atoms which are riding their parent atoms with an isotropic temperature factor arbitrarily chosen as 1.2 times that of the respective parent. Final $R(F)$, $wR(F^2)$ and goodness of fit agreement factors, details on the data collection and analysis can be found in Table 3.

Table 3. Crystallographic data for complexes **1**–**3**.

	1	**2**	**3**
Empirical formula	$C_{30}H_{31}ClN_{24}Ni_2MnO_{19}$	$C_{30}H_{30}ClN_{24}Ni_2FeO_{19}$	$C_{41}H_{74}N_{25}Ni_2O_{20}Tb$
M /g mol^{-1}	1239.60	1239.50	1513.59
T / K	100(2)	120(2)	100(2)
λ / Å	1.54178	1.54178	0.71073
Crystal system	monoclinic	monoclinic	monoclinic
Space group	$P2_1/c$ (14)	$P2_1/c$ (14)	$C2/c$ (15)
a / Å	12.6095(7)	12.5502(14)	28.2544(5)
b / Å	17.3925(10)	17.4452(19)	19.0526(2)
c / Å	22.9337(13)	23.095 (3)	24.6534(9)
α / °	90	90	90
β / °	105.209(3)	105.212(7)	147.1680(10)
γ / °	90	90	90
V / Å^3	4853.4(5)	4879.4(10)	7195.5(3)
Z	4	4	4
ρ / g cm^{-3}	1.696	1.687	1.397
μ / mm^{-1}	4.368	4.624	1.568
Unique reflections	60200	60945	27956
R_{int}	0.0780	0.1053	0.0331
GOF on F^2	1.018	1.042	1.107
R_1[a] [$I > 4\sigma(I)$]	0.0529	0.0532	0.0306[b]
wR_2[a] [$I > 4\sigma(I)$]	0.1292	0.1289	0.1075

[a] $R(F) = \sum||F_o| - |F_c||/\sum|F_o|$, $wR(F^2) = [\sum w(F_o^2 - F_c^2)^2/\sum wF^4]1/2$. [b] SQUEEZE.

CCDC-832384 (for **1**), -832385 (for **2**), -832386 (for **3**) contain the supplementary crystallographic data. These data can be obtained free of charge from The Cambridge Crystallographic Data Centre via www.ccdc.cam.ac.uk/data_request/cif.

Supporting Information (see footnote on the first page of this article): Synthesis and structure of the mononuclear complex $[Ni(H_2L)_3]F(ClO_4){\cdot}CH_3OH{\cdot}H_2O$.

Acknowledgments

This work was supported by the Spanish Ministerio de Educación y Ciencia (MEC) (project CTQ-2008-02269/BQU), the Junta de Andalucía (FQM-195 and Projects of Excellence P08-FQM-03705) and the University of Granada. M. A. P. thanks the Spanish Ministerio de Ciencia e Innovación (MICINN) for a FPI grant. Financial support from the University of Granada and Junta de Andalucia for the visit of E. C. at the University of Edinburgh is grateful acknowledged. We would like to thank the Centro de Supercomputación de la Universidad de Granada for computational resources and Dr. Joan Cano, University of Valencia, Spain, for his continuous and generous assistance with the DFT calculations. E. K. B would also like to thank the Engineering and Physical Sciences Research Council (EPSRC) and Leverhulme Trust for financial support.

[1] a) P. Chaudhuri, *Coord. Chem. Rev.* **2003**, *243*, 143; b) C. J. Milios, T. C. Stamatatos, S. P. Perlepes, *Polyhedron* **2006**, *25*, 134; c) C. J. Milios, S. Piligkos, E. K. Brechin, *Dalton Trans.* **2008**, 1809. V. Yu. Kukushkin, A. J. L. Pombeiro, *Coord. Chem. Rev.* **1999**, *181*, 147. A. G. Smith, P. A. Tasker, D. J. White, *Coord. Chem. Rev.* **2003**, *241*, 61.

[2] a) T. C. Stamatatos, D. Foguet-Albiol, S.-C. Lee, C. C. Stoumpos, C. P. C. P. Raptopoulou, A. Terzis, W. Wernsdorfer, S. O. Hill, S. P. Perlepes, G. Christou, *J. Am. Chem. Soc.* **2007**,

129, 9484; b) T. C. Stamatatos, D. Foguet-Albiol, S.-C. Lee, C. C. Stoumpos, C. P. C. P. Raptopoulou, A. Terzis, W. Wernsdorfer, S. O. Hill, S. P. S. Perlepes, G. Christou, *Polyhedron* **2007**, *26*, 2165; c) S.-C. Lee, T. C. Stamatatos, S. Hill, S. P. Perlepes, G. Christou, *Polyhedron* **2007**, *26*, 2225.
[3] C. Coulon, H. Miyasaka, R. Clérac, *Struct. Bonding (Berlin)* **2006**, *122*, 163; H. Miyasaka, M. Julve, M. Yamashita, R. Clérac, *Inorg. Chem.* **2009**, *48*, 3420.
[4] a) C. Papatriantafyllopoulou, L. F. Jones, T. D. Nguyen, N. Matamoros-Salvador, L. Cunha-Silva, F. A. Almeida Paz, J. Rocha, M. Evangelisti, E. K. Brechin, S. Perlepes, *Dalton Trans.* **2008**, 3153; b) C.-M. Ji, H.-J. Yang, C.-C. Zhao, V. Tangoulis, A.-L. Cui, H.-Z. Kou, *Cryst. Growth Des.* **2009**, *9*, 4607–4609; c) H.-Z. Kou, G.-Y. An, C.-M. Ji, B.-W. Wang, A.-L. Cui, *Dalton Trans.* **2010**, *39*, 9604–9610; d) G.-Y. An, C.-M. Ji, A.-L. Cui, H.-Z. Kou, *Inorg. Chem.* **2011**, *50*, 1079–1083.
[5] M. A. Palacios, A. J. Mota, J. E. Perea-Buceta, F. J. White, E. K. Brechin, E. Colacio, *Inorg. Chem.* **2010**, *49*, 10156.
[6] B. Gole, R. Chakrabarty, S. Mukherjee, Y. Song, P. S. Mukherjee, *Dalton Trans.* **2010**, *39*, 9766.
[7] a) T. Weyhermüller, R. Wagner, S. Khanra, P. Chaudhuri, **2005**, 2539; b) P. Chaudhuri, T. Weyhermüller, R. Wagner, S. Khanra, B. Biswas, E. Bothe, E. Bill, *Inorg. Chem.* **2007**, *46*, 2010.
[8] a) T. C. Stamatatos, A. Bell, P. Cooper, A. Terzis, C. P. Raptopoulou, S. L. Heath, R. E. P. Winpenny, S. P. Perlepes, *Inorg. Chem. Commun.* **2005**, *8*, 533; b) T. C. Stamatatos, A. Bell, P. Cooper, A. Terzis, C. P. Raptopoulou, S. L. Heath, R. E. P. Winpenny, S. P. Perlepes, *Polyhedron* **2009**, *28*, 1638.
[9] C. Papatriantafyllopoulou, M. Estrader, C. G. Efthymiou, D. Dermitzaki, K. Gkotsis, A. Terzis, C. Diaz, S. P. Perlepes, *Polyhedron* **2009**, *28*, 1652.
[10] M. Llunell, D. Casanova, J. Cirera, J. M. Bofill, P. Alemany, S Alvarez, M. Pinsky, D. Avnir, *SHAPE*, version 1.1b, Barcelona, **2005**.
[11] I. B. Bersuker, in: *Electronic Structure and Properties of Transition Metal Compounds, Introduction to the theory*, John Wiley & Sons, New York, **1996**, p. 292–336.
[12] For some examples, see: a) D. Lundberg, I. Persson, L. Eriksson, P. D'Angelo, S. De Panfilis, *Inorg. Chem.* **2010**, *49*, 4420; b) Q. Yue, J. Yang, G.-H. Li, G.-D. Li, J.-S. Chen, *Inorg. Chem.* **2006**, *45*, 4431.
[13] MAGMUN 4.0/OW0L is available as a combined package free of charge from the authors at http://www.ucs.mun.ca/lthomp/. MAGMUN has been developed by Dr. Z. Xu, and L. K. Thompson, (Memorial University), and OW01.exe, by Dr. O. Waldmann, (University of Bern). The software calculates the total spin state values (*S*) and their associated energies (*E*) using the Kambe approach and then substitutes the S and E values into the van Vleck equation to generate the variable-temperature susceptibility profile (degenerate states are accounted for).
[14] C. J. Milios, E. Kefalloniti, C. P. Raptopoulou, A. Terzis, A. Escuer, R. Vicente, S. P. Perlepes, *Polyhedron* **2004**, *23*, 83; F. Birkelbach, U. Flörke, H.-J. Haupt, C. Butzlaff, A. X. Trautwein, K. Wieghardt, P. Chaudhuri, *Inorg. Chem.* **1998**, *37*, 2000.
[15] C. Benelli, D. Gatteschi, *Chem. Rev.* **2002**, *102*, 2369, and references cited therein. J. P. Sutter, O. Kahn, *Magnetism: Molecules to Materials* (Eds.: J. S. Miller, M. Drillon), Wiley-VCH, Weinheim, Germany, **2005**, vol. V, p. 161.
[16] O. Kahn, *Molecular Magnetism*, VCH, Weinheim, Germany, **1993**.
[17] F. Z. C. Fellah, J. P. Costes, F. Dahan, C. Duhayon, G. Novitchi, J. P. Tuchagues, L. Vendier, *Inorg. Chem.* **2008**, *47*, 6444.
[18] T. Kajiwara, M. Nakano, K. Takahashi, S. Takaishi, M. Yamashita, *Chem. Eur. J.* **2011**, *17*, 196.
[19] R. J. Blagg, C. A. Muryn, E. J. L. McInnes, F. Tuna, R. E. P. Winpenny, *Angew. Chem. Int. Ed.* **2011**, *50*, 6530 and references cited therein.
[20] E. Colacio, J. Ruiz-Sanchez, F. J. White, E. K. Brechin, *Inorg. Chem.* **2011**, *50*, 7268, and references cited therein.
[21] J. Long, F. Habib, P.-H. Lin, I. Korobkov, G. Enright, L. Ungur, W. Wernsdorfer, L. F. Chibotaru, M. Murugesu, *J. Am. Chem. Soc.* **2011**, *133*, 5319, and references cited therein.
[22] A. Rodríguez-Diéguez, R. Kivekäs, H. Sakiyama, A. Debdoubi, E. Colacio, *Dalton Trans.* **2007**, *46*, 2503.
[23] a) A. D. Becke, *Phys. Rev. A* **1988**, *38*, 3098; b) C. Lee, W. Yang, R. G. Parr, *Phys. Rev. B 37* **1988**, 785; c) A. D. Becke, *J. Chem. Phys.* **1993**, *98*, 5648.
[24] M. J. Frisch, G. W. Trucks, H. B. Schlegel, G. E. Scuseria, M. A. Robb, J. R. Cheeseman, J. A. Montgomery Jr, T. Vreven, K. N. Kudin, J. C. Burant, J. M. Millam, S. S. Iyengar, J. Tomasi, V. Barone, B. Mennucci, M. Cossi, G. Scalmani, N. Rega, G. A. Petersson, H. Nakatsuji, M. Hada, M. Ehara, K. Toyota, R. Fukuda, J. Hasegawa, M. Ishida, T. Nakajima, Y. Honda, O. Kitao, H. Nakai, M. Klene, X. Li, J. E. Knox, H. P. Hratchian, J. B. Cross, C. Adamo, J. Jaramillo, R. Gomperts, R. E. Stratmann, O. Yazyev, A. J. Austin, R. Cammi, C. Pomelli, J. W. Ochterski, P. Y. Ayala, K. Morokuma, G. A. Voth, P. Salvador, J. J. Dannenberg, V. G. Zakrzewski, S. Dapprich, A. D. Daniels, M. C. Strain, O. Farkas, D. K. Malick, A. D. Rabuck, R. Raghavachari, J. B. Foresman, J. V. Ortiz, Q. Cui, A. G. Baboul, S. Clifford, J. Cioslowski, B. B. Stefanov, G. Liu, A. Liashenko, P. Piskorz, I. Komaromi, R. L. Martin, D. J. Fox, T. Keith, M. A. Al-Laham, C. Y. Peng, A. Nanayakkara, M. Challacombe, P. M. W. Gill, B. Johnson, W. Chen, M. W. Wong, C. Gonzalez, J. A. Pople, *Gaussian 03*, revision E.01, Gaussian, Inc., Wallingford CT, **2004**.
[25] G. B. Bacskay, *Chem. Phys.* **1981**, *61*, 385.
[26] A. Schaefer, C. Huber, R. Ahlrichs, *J. Chem. Phys.* **1994**, *100*, 5829.
[27] *Jaguar 7.6*, Schrödinger, Inc., Portland OR, **2009**.
[28] a) E. Ruiz, J. Cano, S. Alvarez, P. Alemany, *J. Comput. Chem.* **1999**, *20*, 1391; b) E. Ruiz, S. Alvarez, A. Rodríguez-Fortea, P. Alemany, Y. Puoillon, C. Massobrio, in: *Magnetism: Molecules to Materials* (Eds.: J. S. Miller, M. Drillon), Wiley-VCH, Weinheim, Germany, **2001**, vol. II, p. 5572; c) E. Ruiz, S. Alvarez, J. Cano, V. Polo, *J. Chem. Phys.* **2005**, *123*, 164110.
[29] G. M. Sheldrick, *SADABS*, University of Göttingen, Germany, **2002**.
[30] *Bruker Apex2*, Bruker AXS Inc, Madison, Wisconsin, USA, **2004**.
[31] *CrysAlisPro Software system*, v. 1.171.33.55, Supernova CCD system, Oxford Diffraction Ltd., Oxford, **2007**.
[32] A. Altomare, M. Cascarano, C. Giacovazzo, A. Guagliardi, M. C. Burla, G. Pilodori, M. Camalli, *J. Appl. Crystallogr.* **1994**, *27*, 435.
[33] G. M. Sheldrick, *SHELX97: Program for Crystal Structure Refinement*, University of Göttingen, Germany, **1997**.
[34] A. L. Spek, *PLATON-94*, v. 101094, *A Multipurpose Crystallographic Tool*, University of Utrecht, The Netherlands, **1994**.

Received: July 8, 2011
Published Online: November 4, 2011

